



A semiconducting gyroidal metal-sulfur framework for chemiresistive sensing†

Cite this: *J. Mater. Chem. A*, 2017, 5, 16139

Received 7th March 2017
Accepted 20th April 2017

DOI: 10.1039/c7ta02069d

rsc.li/materials-a

Jiahong Huang,^a Yonghe He,^a Ming-Shui Yao,^b Jun He,^{*a} Gang Xu,^{ID *b}
Matthias Zeller^c and Zhengtao Xu^{*d}

The gyroid is an iconic structure that conjures up an intriguing 3D congener of the famous electronic systems of graphene and related 2D materials. Unlike the more accessible 2D graphitic systems, gyroidal metal-organic frameworks with demonstrated conductive properties remain unknown. We here report a semiconducting gyroidal net (denoted as HTT-Pb) that derives its rich electronic properties from the large organic π -electron system of a triphenylene core, highly polarizable Pb-dithiolene links, and robust Pb-oxo connections. In contrast to the generally encountered difficulty in crystallizing metal-thiolate networks, single crystals of HTT-Pb amenable to X-ray studies can be reliably obtained by regular solvothermal synthesis. The electronic conductivity of the framework solid is highly responsive to the water content in air, demonstrating potential use in chemiresistive sensing of humidity.

The gyroid (G-surface) belongs to a family of triply periodic minimal surfaces (TPMSs): it divides space into two equivalent, interwoven channel domains and has everywhere a uniform saddle shape with zero mean curvature ($k_1 + k_2 = 0$) and negative Gaussian curvature ($k_1 k_2 < 0$; k_1 and k_2 being the two principal curvatures). In addition to its frequent occurrence in various materials systems (*i.e.*, liquid crystals, block copolymers, and solid state inorganics and frameworks),¹ electronic properties associated with the gyroid and other minimal surfaces (*e.g.*, Schwarz P

and D surfaces) have of late attracted increasing interest. For example, structural modeling indicates that these surfaces can be tiled with carbon polygons to generate carbon schwarzites (or Mackay-Terrones crystals) as 3D analogs of intensely studied graphene sheets. Since the initial proposition in 1991,² numerous theoretical studies have been conducted to reveal the remarkable stability and potentially intriguing electronic properties of these negatively curved graphitic carbon networks;³ the making of these 3D all-carbon crystals has, however, remained a challenge, and only illusive, sporadic occurrence has been reported so far. One major difficulty here lies in the very strong constituent C-C bond that frustrates the assembly of extended ordered structures, while negatively curved molecules⁴ as discrete fragments of these carbon networks are well known.

The synthetic obstacle to all-carbon nets prompts us to target more accessible systems of solid state materials for the exploration of electronic properties in association with 3D minimal surfaces. For this, the structural and functional versatility of intensely studied metal-organic frameworks (MOFs) can be advantageous.⁵ Unlike the intractable C-C bond for carbon schwarzites, the very diverse metal-organic links offer a broad range of bonding strengths to help accommodate the formation of ordered solid state networks. Also, networks of a selected topology (connectivity) can be assembled with a certain degree of correlation with the shapes of the organic linkers and the metal nodes. Notably, networks with structures associated with minimal surfaces have since long been of interest in the MOF field.^{18,6} For example, rigid tritopic molecules can sometimes link up with metal nodes to generate a 3-connected net that is of the gyroid topology [*i.e.*, a (10,3)-a net].^{6a,b}

Electrical conductivity, however, remains unexplored for gyroidal MOF solids. In general, the largely insulating characters of MOF solids arise from the weak electronic interaction across the molecular units,⁷ and polarizable ligands and metal centers are often used to enhance charge transport.⁸ Among these, metal-thiolate links figure prominently,⁹ while strong metal-amine and metal-aryloxide bonds have also been explored.¹⁰ Our long-standing efforts to access semiconductive

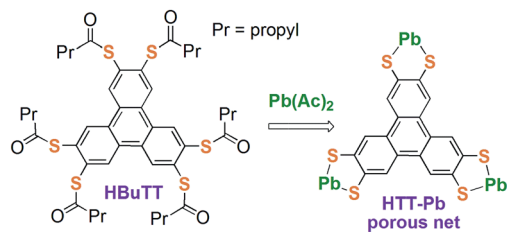
^aSchool of Chemical Engineering and Light Industry, Guangdong University of Technology, Guangzhou 510006, Guangdong, China. E-mail: junhe@gdut.edu.cn

^bState Key Laboratory of Structural Chemistry, Fujian Institute of Research on the Structure of Matter, Chinese Academy of Sciences, Fuzhou 350002, Fujian, China. E-mail: gxu@fjirsm.ac.cn

^cDepartment of Chemistry, Purdue University, 560 Oval Drives, West Lafayette, Indiana, 47907 USA

^dDepartment of Biology and Chemistry, City University of Hong Kong, 83 Tat Chee Avenue, Kowloon, Hong Kong, China. E-mail: zhengtao@cityu.edu.hk

† Electronic supplementary information (ESI) available: Experimental details and general procedures; XRD, IR, Raman, EPR, XPS, TGA, optical absorption spectrum and temperature dependent *I-V* curves. CCDC 1506170 contains the supplementary crystallographic data for HTT-Pb. For ESI and crystallographic data in CIF or other electronic format see DOI: 10.1039/c7ta02069d



Scheme 1 Synthesis of the HTT–Pb framework solid.

networks^{7b,11} utilize polycyclic aromatic linkers (like in HTT, 2,3,6,7,10,11-triphenylene hexathiol)^{9a,10a,12} not only as a source of highly polarizable π -electrons, but also as incipient fragments of the above carbon schwarzites. Like the carbon schwarzites, the strong metal–ligand links here hinder the growth of ordered networks, and consequently, only polycrystalline powders or less-ordered solids were obtained. For instance, a recent semiconductive MOF based on HTT and Pt(II) features a 2D kagome lattice with distinct electronic properties, but only polycrystalline samples with small grain sizes were obtained.⁹ⁱ

This is what makes the present single crystal structure so worthy of note. This is a 3D network based on the dithiolene

linker HTT and Pb(II) ions (denoted as HTT–Pb). Besides its highly ordered structure and tunable semiconductive properties, its gyroidal topology represents a solid step toward the synthesis and exploration of electronic systems related to periodic minimal surfaces.

A solvothermal reaction (Scheme 1) of 2,3,6,7,10,11-hexakis(butyrylthio)triphenylene (HBUtt), Pb(OAc)₂ (OAc: acetate) and NaOH in a mixed solvent of ethylenediamine (EDA) and methanol at 95 °C yielded light-orange crystals of HTT–Pb. HTT–Pb features a formula [Pb₃OH_{0.5}(HTT)]^{1.5-} for the anionic framework, with the negative charge being balanced by the cations in the channel (*e.g.*, EDX analysis indicated substantial presence of Na⁺). The HBUtt molecules under the reaction conditions hydrolyse *in situ* to form the HTT thiol species (Scheme S1†): as a masked version of HTT, HBUtt thus serves to slow down the reaction between the sulfur groups and the Pb(II) ions, to promote crystallization as a result. By comparison, if the free thiol of HTT is directly mixed with the Pb(OAc)₂ solution, an amorphous precipitate was formed immediately, and no significant improvement in crystallinity was observed even after prolonged heating.

Single-crystal X-ray diffraction revealed that HTT–Pb crystallizes in the cubic space group *Pa* $\bar{3}$. The asymmetric portion of the unit cell contains 1/3 of an O atom, one Pb(II) center and 1/3

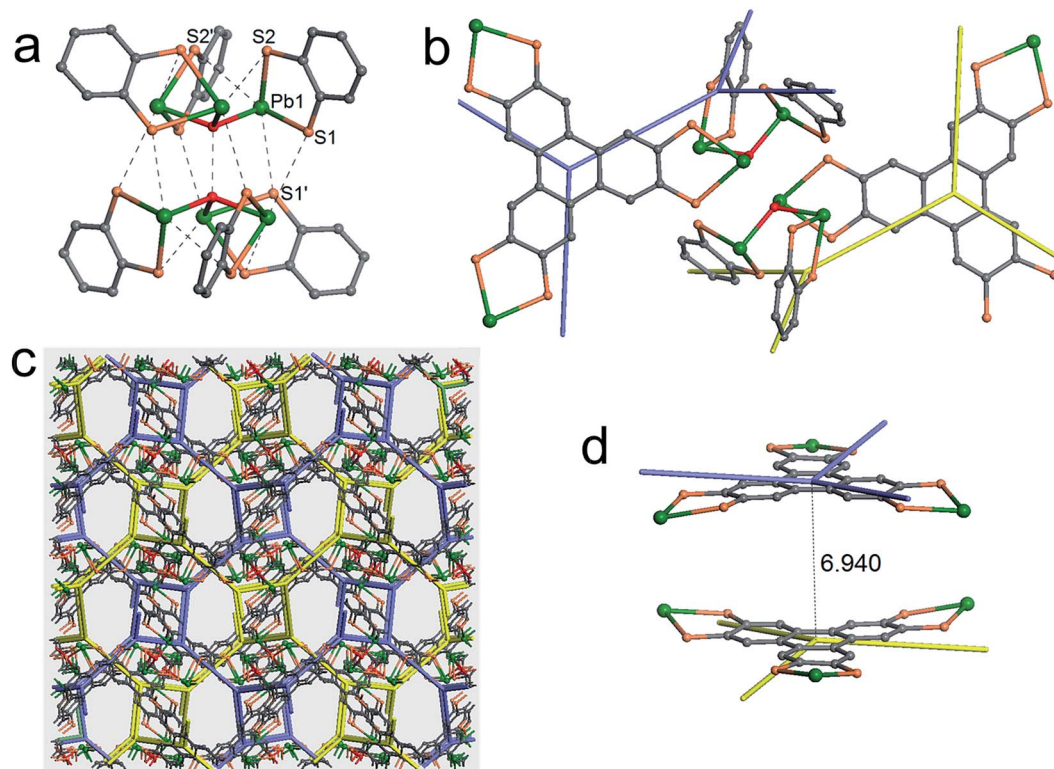


Fig. 1 Single crystal structure of HTT–Pb. (a) The coordination environment around a pair of Pb₃(μ_3 -O) units; only one benzenoid ring of the triphenylene unit is shown; the secondary interactions are shown as dashed lines. Interatomic distances (Å): Pb1–S1, 2.714; Pb1–S2, 2.666; Pb1–S1', 3.666; Pb1–S2', 3.258; the O...O contact is 2.659 Å. (b) Two HTT linkers bonded to a Pb₃(μ_3 -O) pair, together with the topological representation shown as fragments of two interpenetrating 3-connected, gyroidal nets (shown in yellow and purple, respectively). (c) An overview of the single crystal structure of HTT–Pb with the two corresponding gyroidal nets. (d) Two parallel HTT linker molecules, each from a separate gyroidal net, together with their topological equivalents (in yellow and purple, respectively). Pb atoms: green; S: orange; C: grey; O: red.

of an HTT ligand. The O atom is bonded to three crystallographically equivalent Pb(II) centers (Pb–O distance: 2.301 Å; Pb–O–Pb angle: 110.0°) to form a $\text{Pb}_3(\mu_3\text{-O})$ core with the shape of a squashed trigonal pyramid (Fig. 1a). The Pb–O distance is quite short, similar to those found in the crystal structure of PbO ,¹³ wherein the short Pb–O distances generate substantial semiconductive attributes in the solid state. The Pb(II) ion is also chelated to two S atoms of HTT with characteristic covalent Pb–S distances of 2.666 and 2.714 Å. The trigonal $\text{Pb}_3(\mu_3\text{-O})$ core, together with the tritopic HTT linker, generates a three-connected network of the gyroid topology (srs net; Fig. 1b and c).

The inorganic node of the srs net, *i.e.*, the $\text{Pb}_3(\mu_3\text{-O})$ core, pairs up *via* distinct intermolecular interactions (Fig. 1a and b). The two Pb_3O pyramids are related by the 3_1 screw axis, and the two O apices are only 2.7 Å apart, indicating an O–H \cdots O hydrogen bonding interaction. In addition, the two Pb_3O pyramids are also linked by three symmetry-related Pb \cdots S secondary interactions (*i.e.*, Pb \cdots S1) at 3.507 Å. The Pb center is also in contact with two other S atoms (Pb \cdots S distances: 3.258, 3.666 Å); these two sulfur atoms being chelated to another Pb center within the same Pb_3O unit, and they do not serve to link up across the two Pb_3O pyramids.

Two interpenetrating gyroid nets were found in the crystal structure of HTT–Pb, each residing in one of the two channel domains molded by the gyroid surface (Fig. 1c). The three-fold symmetry of the HTT triphenylene core, whose centroid lies at the fractional coordinates (0.40, 0.40, 0.40), coincides with the three-fold axis (*e.g.*, the body diagonal of the unit cell) of the gyroid net. Across the two srs nets, distinct pairs of HTT centroids at the distance of 6.94 Å can be identified (Fig. 1d); the corresponding two triphenylene units are staggered, forming a well-defined void that appears to be well-suited for the docking of planar aromatic guests (*i.e.*, to afford an optimal stacking distance of 3.47 Å with the triphenylene flanks).

Powder X-ray diffraction (PXRD) indicates the crystalline phase purity of the HTT–Pb sample (Fig. 2). The HTT–Pb host net remains upstanding after being heated under vacuum at 150 °C (PXRD pattern c in Fig. 2). The HTT–Pb crystals are also

stable in water and common organic solvents (PXRD pattern d in Fig. 2), and can be handled in air for several hours without significant degradation in crystallinity (see Fig. S2† for PXRD patterns; see also Fig. S3† for Raman spectra). With longer exposure to air (*e.g.*, over 24 hours), the light orange, as-made crystals gradually darken, while the crystallinity degrades significantly, as shown by the weaker and broadened PXRD peaks in Fig. S2.† The substantial timeframe (hours) of stability, however, allows electronic properties and device studies to be conducted in air using the as-made sample of HTT–Pb.

Diffuse reflectance measurement of an as-made HTT–Pb solid (Fig. S4†) indicates a band gap of about 1.7 eV, which is smaller than that for most of the semiconducting lead-sulfur-organic network solids.¹⁴ The pressed pellet of HTT–Pb as measured in a two-probe setting exhibits an electrical conductivity of $1.1 \times 10^{-6} \text{ S cm}^{-1}$ at room temperature. Values of the variable-temperature conductivities of the same sample follow the Arrhenius behavior, with an activation energy of 0.396 eV (Fig. S5 and S6†). The low activation energy could be due to the extrinsic resistance—*e.g.*, from contact, grain boundary—being dominant (as compared with the intrinsic resistance of the framework solid), thus obscuring the temperature dependence of the intrinsic, band-like conduction. The electrical conductivity of HTT–Pb compares well with those of other semiconductive metal–sulfur nets.^{9i,14a,15}

The semiconducting HTT–Pb, with its porous network and water stability, suggests chemiresistive application. For this, a moisture sensor device was conveniently fabricated by drop-casting an ethanol suspension of ground HTT–Pb crystals onto an Al_2O_3 substrate with interdigital electrodes.^{10b} The setup for sensing measurement was home-built as schematized in Fig. 3a and S7.† A constant bias potential of 1.0 V was applied *via* a Keithley source meter to the sensor device housed in a gas-flow chamber. Air streams with different relative humidity were achieved by changing the relative rates of dry air flows through a water-filled bubbler and a dry tube, with the actual relative

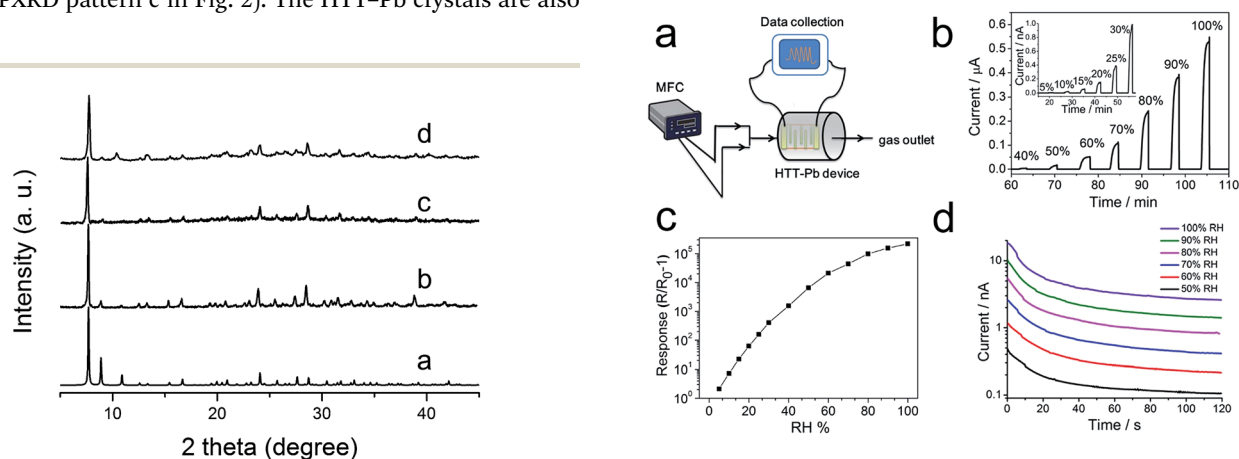


Fig. 2 PXRD patterns (Cu $K\alpha$, $\lambda = 1.5418 \text{ \AA}$): (a) calculated from the single-crystal structure; (b) as-made bulk sample; (c) sample from (b) evacuated by using an oil pump at 150 °C for 1 h; (d) sample from (b) after being soaked in deaerated water at rt for 24 h.

Fig. 3 (a) The homemade setup for the humidity measurement (MFC: mass flow controller); (b) current response of a HTT–Pb based sensor to dry air and different RH (5–100%) at 25 °C; (c) humidity-dependent responses; (d) curves of current vs. time of the HTT–Pb based sensor at various RH obtained by the DC reverse polarity method.

humidity (RH) determined using a commercial humidity sensor. A stable baseline current was observed under flowing dry air; when moist air was mixed in the flow, as shown in Fig. 3b, the electrical current increased rapidly; reverting to dry air, on the other hand, causes the current to drop sharply back to the baseline current within about 6 seconds. Also, a broad, monotonic response ranging from 5 RH% to 100 RH% was observed. The signal strength is also remarkable, e.g. with a baseline current at 10^{-12} A, the conductance increased by over 4 orders of magnitude at 90% RH, with a current as high as 2.7×10^{-7} A (Fig. 3b and c).

To probe electronic and ionic contributions to the moisture-induced increase of electrical conduction, instantaneous polarity reversion was applied to the DC circuit.¹⁶ As high RH generally tends to promote ionic transport, we here choose RH conditions (50% RH–100% RH) to help ascertain the role of ionic conduction. Since electrons move faster than ions, upon reversing the electrical polarity, the ionic current will appear later to form a current peak.¹⁷ The evolution of the current (under different RH conditions) vs. time is shown in Fig. 3d. No peak due to a lagging ionic current was observed and the currents stabilize at 2 to 4 orders (depending on RH) of magnitude larger than the baseline value. Such an observation excludes ions as the major charge carrier, and indicates that the electronic mechanism dominates even under high RH conditions.

Acknowledgements

This work was supported by the National Natural Science Foundation of China (51402293, 21471037 and 61571140), the NSF of Fujian (2015J01230), Guangdong Natural Science Funds for Distinguished Young Scholars (15ZK0307), the Research Fund for the Doctoral Program of Higher Education of China (Grant 201244200120007), and the Research Grants Council of HKSAR [GRF 11303414]. We also thank Prof. Wei-Xiong Zhang at Sun Yat-Sen University and Prof. Qiao-Wei Li at Fudan University for helping with the figures.

Notes and references

- (a) C. Tschierske, *Angew. Chem., Int. Ed.*, 2013, **52**, 8828; (b) K. Borisch, S. Diele, P. Goering, H. Mueller and C. Tschierske, *Liq. Cryst.*, 1997, **22**, 427; (c) D. A. Hajduk, P. E. Harper, S. M. Gruner, C. C. Honeker, G. Kim, E. L. Thomas and L. J. Fetters, *Macromolecules*, 1994, **27**, 4063; (d) F. S. Bates and G. H. Fredrickson, *Phys. Today*, 1999, **52**, 32; (e) T. Gier, X. Bu, P. Feng and G. D. Stucky, *Nature*, 1998, **395**, 154; (f) S. Lee, A. B. Mallik, Z. Xu, E. B. Lobkovsky and L. Tran, *Acc. Chem. Res.*, 2005, **38**, 251; (g) X.-P. Zhou, M. Li, J. Liu and D. Li, *J. Am. Chem. Soc.*, 2012, **134**, 67; (h) C. T. Kresge, M. E. Leonowicz, W. J. Roth, J. C. Vartuli and J. S. Beck, *Nature*, 1992, **359**, 710; (i) Z. Xu, S. Lee, E. B. Lobkovsky and Y.-H. Kiang, *J. Am. Chem. Soc.*, 2002, **124**, 121.
- H. Terrones and A. L. Mackay, *Nature*, 1991, **352**, 762.
- T. Lenosky, X. Gonze, M. Teter and V. Elser, *Nature*, 1992, **355**, 333.
- K. Y. Cheung, X. Xu and Q. Miao, *J. Am. Chem. Soc.*, 2015, **137**, 3910.
- (a) J.-R. Li, J. Sculley and H.-C. Zhou, *Chem. Rev.*, 2012, **112**, 869; (b) C. Wang, D. Liu and W. Lin, *J. Am. Chem. Soc.*, 2013, **135**, 13222; (c) Y. Cui, B. Li, H. He, W. Zhou, B. Chen and G. Qian, *Acc. Chem. Res.*, 2016, **49**, 483; (d) J. Jiang, Y. Zhao and O. M. Yaghi, *J. Am. Chem. Soc.*, 2016, **138**, 3255.
- (a) A. B. Mallik, S. Lee and E. B. Lobkovsky, *Cryst. Growth Des.*, 2005, **5**, 609; (b) G. Huang, H. Xu, X.-P. Zhou, Z. Xu, K. Li, M. Zeller and A. D. Hunter, *Cryst. Growth Des.*, 2007, **7**, 2542; (c) Y. Wu, X.-P. Zhou, J.-R. Yang and D. Li, *Chem. Commun.*, 2013, **49**, 3413; (d) F. Wang, H.-R. Fu and J. Zhang, *Cryst. Growth Des.*, 2015, **15**, 1568; (e) X. Luo, Y. Cao, T. Wang, G. Li, J. Li, Y. Yang, Z. Xu, J. Zhang, Q. Huo, Y. Liu and M. Eddaoudi, *J. Am. Chem. Soc.*, 2016, **138**, 786.
- (a) Z. Xu, *Coord. Chem. Rev.*, 2006, **250**, 2745; (b) Z. Xu, *Met.-Org. Framework Mater.*, 2014, 373; (c) L. Sun, M. G. Campbell and M. Dincă, *Angew. Chem., Int. Ed.*, 2016, **55**, 3566.
- (a) K. M. Hutchins, T. P. Rupasinghe, L. R. Ditzler, D. C. Swenson, J. R. G. Sander, J. Baltrusaitis, A. V. Tivanski and L. R. MacGillivray, *J. Am. Chem. Soc.*, 2014, **136**, 6778; (b) A. A. Talin, A. Centrone, A. C. Ford, M. E. Foster, V. Stavila, P. Haney, R. A. Kinney, V. Szalai, F. El Gabaly, H. P. Yoon, F. Léonard and M. D. Allendorf, *Science*, 2014, **343**, 66; (c) T. Neumann, J. Liu, T. Wächter, P. Friederich, F. Symalla, A. Welle, V. Mugnaini, V. Meded, M. Zharnikov, C. Wöll and W. Wenzel, *ACS Nano*, 2016, **10**, 7085; (d) Z. Zhang, H. Zhao, H. Kojima, T. Mori and K. R. Dunbar, *Chem.-Eur. J.*, 2013, **19**, 3348; (e) Z. Zhang, H. Yoshikawa and K. Awaga, *J. Am. Chem. Soc.*, 2014, **136**, 16112.
- (a) Y. Zhao, M. Hong, Y. Liang, R. Cao, J. Weng, S. Lu and W. Li, *Chem. Commun.*, 2001, 1020; (b) W. Su, M. Hong, J. Weng, R. Cao and S. Lu, *Angew. Chem., Int. Ed.*, 2000, **39**, 2911; (c) X.-Y. Tang, H.-X. Li, J.-X. Chen, Z.-G. Ren and J.-P. Lang, *Coord. Chem. Rev.*, 2008, **252**, 2026; (d) S. Takaishi, M. Hosoda, T. Kajiwara, H. Miyasaka, M. Yamashita, Y. Nakanishi, Y. Kitagawa, K. Yamaguchi, A. Kobayashi and H. Kitagawa, *Inorg. Chem.*, 2009, **48**, 9048; (e) Y. Kobayashi, B. Jacobs, M. D. Allendorf and J. R. Long, *Chem. Mater.*, 2010, **22**, 4120; (f) K.-H. Low, V. A. L. Roy, S. S.-Y. Chui, S. L.-F. Chan and C.-M. Che, *Chem. Commun.*, 2010, **46**, 7328; (g) T. Kambe, R. Sakamoto, K. Hoshiko, K. Takada, M. Miyachi, J.-H. Ryu, S. Sasaki, J. Kim, K. Nakazato, M. Takata and H. Nishihara, *J. Am. Chem. Soc.*, 2013, **135**, 2462; (h) E. J. Mensforth, M. R. Hill and S. R. Batten, *Inorg. Chim. Acta*, 2013, **403**, 9; (i) J. Cui and Z. Xu, *Chem. Commun.*, 2014, **50**, 3986; (j) L. Sun, T. Miyakai, S. Seki and M. Dincă, *J. Am. Chem. Soc.*, 2013, **135**, 8185.
- (a) D. Sheberla, L. Sun, M. A. Blood-Forsythe, S. Er, C. R. Wade, C. K. Brozek, A. Aspuru-Guzik and M. Dincă, *J. Am. Chem. Soc.*, 2014, **136**, 8859; (b) M. G. Campbell, D. Sheberla, S. F. Liu, T. M. Swager and M. Dincă, *Angew. Chem., Int. Ed.*, 2015, **54**, 4349; (c) M. Hmadeh, Z. Lu, Z. Liu, F. Gándara, H. Furukawa, S. Wan, V. Agostyn,

- R. Chang, L. Liao, F. Zhou, E. Perre, V. Ozolins, X. Duan, B. Dunn, Y. Yamamoto, O. Terasaki and O. M. Yaghi, *Chem. Mater.*, 2012, **24**, 3511; (d) N. T. T. Nguyen, H. Furukawa, F. Gándara, C. A. Trickett, H. M. Jeong, K. E. Cordova and O. M. Yaghi, *J. Am. Chem. Soc.*, 2015, **137**, 15394.
- 11 (a) K. Li, Z. Xu, H. Xu and J. M. Ryan, *Chem. Mater.*, 2005, **17**, 4426; (b) K. Li, H. Xu, Z. Xu, M. Zeller and A. D. Hunter, *Inorg. Chem.*, 2005, **44**, 8855; (c) J. He, C. Yang, Z. Xu, M. Zeller, A. D. Hunter and J. Lin, *J. Solid State Chem.*, 2009, **182**, 1821; (d) J. He, M. Zeller, A. D. Hunter and Z. Xu, *CrystEngComm*, 2015, **17**, 9254.
- 12 (a) R. Dong, M. Pfeiffermann, H. Liang, Z. Zheng, X. Zhu, J. Zhang and X. Feng, *Angew. Chem., Int. Ed.*, 2015, **54**, 12058; (b) A. J. Clough, J. W. Yoo, M. H. Mecklenburg and S. C. Marinescu, *J. Am. Chem. Soc.*, 2015, **137**, 118; (c) Z. Xu, K. Li, J. C. Fettinger, J. Li and M. M. King, *Cryst. Growth Des.*, 2005, **5**, 423.
- 13 (a) A. F. Wells, *Structural Inorganic Chemistry*, Clarendon Press, Oxford, 5th edn, 1984; (b) S.-Y. Mao, Y.-P. Mao, M.-P. Zhong and Z.-G. Ye, *J. Alloys Compd.*, 2009, **472**, 328.
- 14 (a) D. L. Turner, T. P. Vaid, P. W. Stephens, K. H. Stone, A. G. DiPasquale and A. L. Rheingold, *J. Am. Chem. Soc.*, 2008, **130**, 14; (b) D. L. Turner, K. H. Stone, P. W. Stephens, A. Walsh, M. P. Singh and T. P. Vaid, *Inorg. Chem.*, 2012, **51**, 370.
- 15 L. Sun, C. H. Hendon, M. A. Minier, A. Walsh and M. Dincă, *J. Am. Chem. Soc.*, 2015, **137**, 6164.
- 16 K. Jiang, T. Fei, F. Jiang, G. Wang and T. Zhang, *Sens. Actuators, B*, 2014, **192**, 658.
- 17 K. Jiang, H. Zhao, T. Fei, H. Dou and T. Zhang, *Sens. Actuators, B*, 2016, **222**, 440.